Compton profiles of lutetium and lutetium dihydride

R. Lässer and B. Lengeler
Institut für Festkörperforschung, Kernforschungsanlage Jülich, 5170 Jülich, Germany

K. A. Gschneidner, Jr. and P. Palmer
Ames Laboratory—DOE and Department of Materials Science and Engineering, Iowa State University, Ames, Iowa 50011

(Received 26 January 1979)

Compton profiles for polycrystalline Lu and $LuH_{2.05}$ have been determined by Compton scattering of 320-keV photons from a ^{51}Cr source. The profiles for pure Lu have been corrected for multiple scattering and compared to a renormalized-free-atom model for the conduction electrons. The Compton profile for metallic Lu suggests an electronic configuration close to $5d^16s^2$. A model for the dihydride based on a band-structure calculation by Switendick in which a new band of antibonding hydrogen wave functions accommodates the two extra electrons per LuH_2 explains the experimental Compton profile in a satisfactory way.

I. INTRODUCTION

Compton scattering has been used extensively over the last years to measure the electron momentum distribution in metals and alloys.[1] Most investigations have been done on low-Z elements and their compounds. In this paper we report on the measurements of Compton profiles and on the calculation of electron momentum distributions of the heavy lanthanide element lutetium ($Z=71$) and its dihydride. With appropriate precautions in the experimental design we were able to measure absolute Compton profiles even in this high-Z element. This is of great interest for the investigation of the electronic structure of metallic Lu because other standard techniques such as the de Haas–van Alphen effect have not been successfully applied to this metal because of difficulties in preparing adequate single crystals of sufficiently high purity. Although Hoekstra and Phillips[2] have observed de Haas–van Alphen oscillations in lutetium these have been insufficient to map out the Fermi surface. The experimental results have been compared with a model for the electron momentum distribution which is based on a renormalized-free-atom (RFA) approximation for the Bloch functions.[3,4]

Of all elements the rare earths are among those which dissolve the most hydrogen, and most of the rare-earth metals form hydrides containing 2 and 3 hydrogen atoms per metal atom.[5] The structures of the different hydrides show certain regularities which have been explained by Switendick[6] by means of an APW (augmented plane-wave) band-structure calculations. The main result of these calculations for the cubic dihydrides, which have the CaF_2 structure, is that a new band forms below the Fermi level which is an antibonding hybrid of the two $1s$ hydrogen orbitals on the two tetrahedral sites. This new band is responsible for the stability of the dihydrides. Its position is largely determined by the hydrogen-hydrogen distance. It can accommodate two electrons per atom. Therefore, the Fermi level is practically unchanged in the dihydride compared to that in the pure metal. However, the electronic density of states at the Fermi level is lowered considerably (by a factor ~ 10).[7] It is one of the purposes of this investigation to check these results by Compton scattering for LuH_2 which has also the CaF_2 structure.

II. EXPERIMENTAL

The experimental set-up used in this investigation is similar to the one described in Ref. 8. The main changes are the following: we have used here the isotope ^{51}Cr, emitting 320.076-keV photons,[9] with a half-life of 27.8 days. The source has a spherical shape of 3 mm in diameter prepared from 90% enriched ^{50}Cr and had an activity of 83 Ci after neutron activation. The small size of the source and its mounting between two thin aluminum foils keeps the scattering of photons in the source and its support small. We have used cylindrical beam channels in the present set-up. The mean scattering angle was 173.0°. The detector resolution was 537 eV full width at half maximum (FWHM) at the energy of the Compton peak (142.38 keV at 173°). The angular divergence of the beam deteriorated the resolution by 4.5% resulting in a total resolution of 561 eV FWHM or 0.375 a.u. (Ref. 10). In order to keep the background scattering small the source and the backscattering channel were separated by a 14 mm thick

TABLE I. Chemical analysis of the lutetium in atomic ppm (the concentrations of the elements not listed are <1 ppm)

Impurity	Conc.	Impurity	Conc.
H	693	Ni	8
C	233	Cu	10
N	25	La	1.7
O	403	Nd	2.4
F	<27	Gd	<4
Na	6	Hf	<2
Si	1.2	Ta	4.5
Cl	2	W	67
Cr	2.6	Os	<5
Fe	15.6		

tungsten plate. The samples were suspended by needles in an evacuated sample chamber, the walls of which were clad with lead foil.

The Lu samples were prepared at the Ames Laboratory, Iowa State University in the form of 0.5 and 2.0 mm thick polycrystalline platelets. The chemical analysis of the starting material is given in Table I. The hydrogen loading of the samples was carried out in a high vacuum ($\sim 10^{-7}$ Torr) system. After the samples had been heated to 600 °C a known amount of hydrogen gas, which was purified in a palladium cell, was let into the system. The samples were kept at that temperature for two hours and then cooled down slowly to room temperature. The hydrogen concentration was also verified by heat extraction. Hydrides with a composition $LuH_{2.05}$ were prepared. The internal stresses introduced by the hydrogen loading caused many cracks in the samples. The thin (0.5 mm) samples fell apart into a few pieces whereas the 2 mm sample remained as one piece. Thus, Compton profiles for $LuH_{2.05}$ were measured only on 2 mm samples but for Lu they were measured on samples of 0.5 and 2 mm thickness. In order to avoid oxidation the samples were stored in argon or in vacuum.

III. RESULTS

Figure 1 shows the energy distribution of the Compton scattered photons for $LuH_{2.05}$ and Lu. About 10^5 counts per channel (83.2 eV) were collected in 2.8 days at the Compton peak. The signal-to-noise ratio was 83. In order to compare the two distributions the data for Lu have been adjusted at 154 keV to the same number of counts per channel as were in the $LuH_{2.05}$ distribution at that energy. It should be noted that the core contributions for both samples agree very well and that the hydrogen affects only the electron momenta between −3 and +3 a.u. The profiles are very symmetric. This is, among others, a consequence of the cleaness of the ^{51}Cr source in which Compton scattering is kept small so that only 320-keV photons hit the sample. In addition,

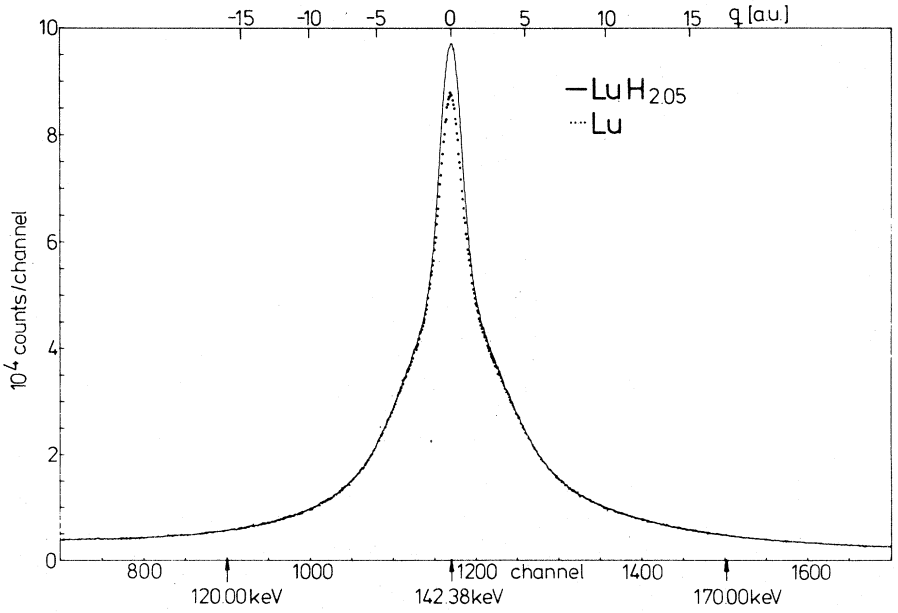

FIG. 1. Energy distribution of 320-keV photons from a ^{51}Cr source scattered under 173° from polycrystalline Lu and $LuH_{2.05}$.

the Ge detector was shielded such that only the central portion (10 mm diameter out of 16 mm crystal diameter) was used to detect the photons. The energy distributions were converted into Compton profiles by the standard scheme[8]: subtraction of a background measured in the set-up without a sample, correction for the detector efficiency, correction for the photon absorption, and for the Compton cross section, transformation of the energy scale into a momentum scale, and normalization of the surface below the Compton profile for the number of electrons per formula unit Lu and $LuH_{2.05}$, respectively. We have used the atomic Compton profiles by Biggs *et al.*[11] The values of the integrals between 0 and 7 a.u. turned out to be 26.357 for Lu and 27.382 for $LuH_{2.05}$. In the case of pure Lu we have made correction for multiple scattering by means of a Monte Carlo program developed by Felsteiner *et al.*[12] In the program the ratio α of the number of multiple scattering events in the Compton profile to the total number of scattering events is calculated as a function of photon energy, sample material, sample dimensions, and beam geometry. The result can be

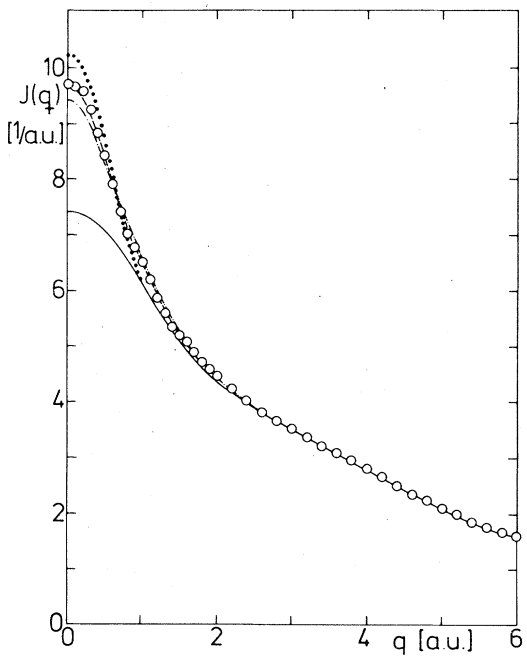

FIG. 2. Compton profile $J(q)$ of polycrystalline Lu corrected for multiple scattering (open circles). Also shown is the profile for the core levels $1s^2 \cdots 4f^{14}$) (full) and the profiles for the configurations $5d^16s^1$ (dashed) and $5d^26s^1$ (dot-dashed) in a RFA model as well as a free-electron model (solid circles). The uncertainty in the experimental data is smaller than the size of the open circles.

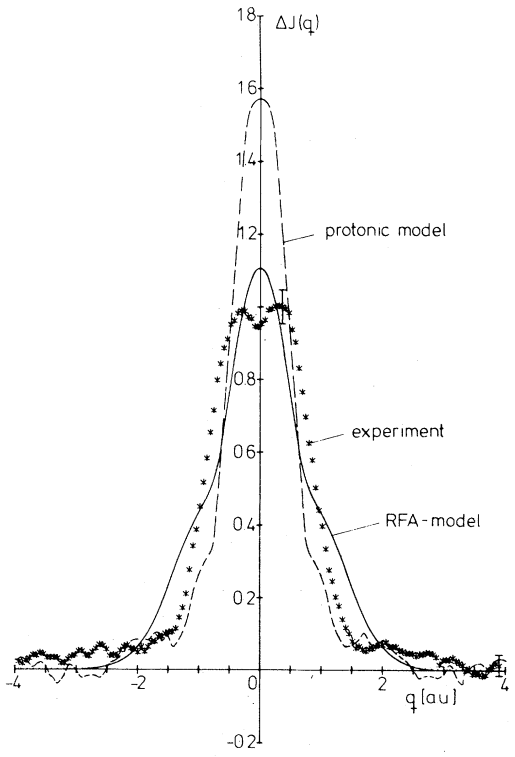

FIG. 3. Difference Compton profile $\Delta J(q)$ between $LuH_{2.05}$ and Lu (stars) compared with a RFA model and a "protonic" model explained in the text.

described to a good approximation by $\alpha = 0.327d/(1+2.08d)$ for a Lu disc of thickness d. Using the measured Compton profiles $J(q,d_1)$ and $J(q,d_2)$ for the two thicknesses $d_1 = 0.5$ mm and $d_2 = 2.0$ mm we have calculated $J(q)$ for thickness zero by linear extrapolation for each individual value of q according to

$$J(q) = \frac{[J(q,d_1)\alpha_2 - J(q,d_2)\alpha_1]}{(\alpha_2 - \alpha_1)} \quad . \tag{1}$$

Here $\alpha_1 = \alpha(d_1 = 0.5) = 0.080$ and $\alpha_2 = \alpha(d_2 = 2.0) = 0.127$. Figure 2 shows the Compton profile for polycrystalline lutetium corrected for multiple scattering.

In the case of $LuH_{2.05}$ we have made no correction for multiple scattering because the profile was measured only for one thickness for the reasons mentioned above. This is not a serious limitation since multiple scattering cancels out to a great extent in the difference profile

$$\Delta J(q) = J_{LuH_{2.05}}(q) - J_{Lu}(q)$$

$\Delta J(q)$ is shown in Fig. 3.

IV. DISCUSSION

We will discuss first the Compton profile for metallic lutetium. In Fig. 2 is plotted the experimental Compton profile for polycrystalline lutetium which has been corrected for multiple scattering but which has not been corrected for the finite energy resolution of the spectrometer. The energy resolution function is a Gaussian

$$g(\omega-\omega') = (2\pi\sigma^2)^{-1/2}\exp[-\hbar^2(\omega-\omega')^2/2\sigma^2] \ , \tag{2a}$$

$$\sigma^2 = (1.7714\hbar\omega + 36730.23)/8\ln 2 \ , \tag{2b}$$

with σ and $\hbar\omega$ given in eV. For comparison of the experimental data with theoretical models we have convoluted the theoretical results with this resolution function after converting the energies $\hbar\omega$ and $\hbar\omega'$ into momenta q and q'.[1]

We have also plotted the Compton profile for the core electrons up to the 14 $4f$ electrons, inclusively, which has been convoluted with the spectrometer resolution function Eq. (2). It is noteworthy that the two profiles agree well with one another above about 2 a.u. This gives us confidence that the experimental set-up and the data analysis are adequate for determining absolute Compton profiles even in high-Z elements. In Table II are listed the values of the Compton profile for polycrystalline lutetium (without correction for the spectrometer resolution). We do not know of any calculations of Compton profiles based on band-structure calculations for Lu. Berko *et al.*[3] and Berggren *et al.*[4] have pointed out that a renormalized-free-atom (RFA) model gives a fair approximation to the electron momentum distribution of electrons in a solid. Therefore, we have applied this model to lutetium using the atomic wave functions for Lu by Herman and Skillman.[13] Lu has a hexagonal lattice with lattice constants $a = 6.6236$ a.u. and $c = 10.4864$ a.u.[14] The unit cell contains two identical atoms and the Wigner-Seitz sphere per atom has a radius of $r_0 = 3.623$ a.u. In the RFA model, approximate wave function for the crystal $\phi_0(\vec{r})$ are derived by truncating the atomic Herman-Skillman wave functions at r_0 and by renormalizing them to 1 per electron within the Wigner-Seitz sphere. It turned out that in Lu 46.9% of the atomic $6s$ electrons are inside the Wigner-Seitz sphere whereas for the $5d$ atomic electrons this number is 88.0%. Since even in a free atom most of the $5d$ electrons are inside the Wigner-Seitz sphere only the $6s$ electrons need to be renormalized. Figure 4 shows the renormalized $6s$ wave function. It should be noted that the boundary condition $d\phi_0(r_0)/dr = 0$ is not satisfied exactly, but according to Berggren[15] the deviation has only a minor influence on the Compton profile. Berggren *et al.*[4] have derived an expression for the isotropic Compton profile in a hexagonal lattice based on the RFA model for s electrons

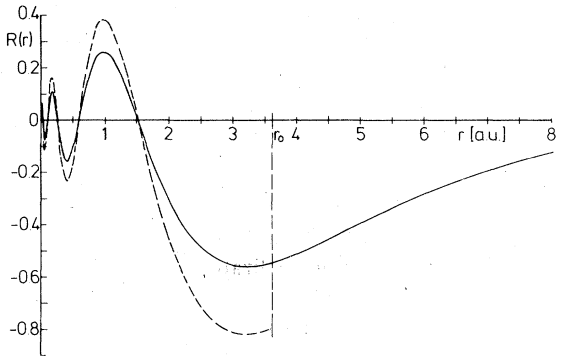

FIG. 4. Hartree-Fock wave functions (solid line) and renormalized free-atom wave function (dashed line) for $6s$ electron in Lu. r_0 is the radius for the Wigner-Seitz sphere of Lu.

$$J_{6s}(q) = 4\pi\sum_{n=0}^{\infty}|\psi_0(K_n)|^2 G_n(q) \ . \tag{3}$$

The sum extends over the different lattice vectors K_n in the reciprocal lattice. $\psi_0(K_n)$ is the Fourier transform of the RFA wave function $\phi_0(\vec{r})$

$$\psi_0(0) = (2/\pi)^{1/2}\int_0^{r_0} dr\, r^2\phi_0(r) \ , \tag{4}$$

$$\psi_0(K_n) = \left(\frac{2}{\pi}\right)^{1/2} K_n^{-1}\int_0^{r_0} dr\, r\sin K_n r\,[\phi_0(r)-\phi_0(r_0)] \ . \tag{5}$$

For $n = 0$

$$G_0(q) = (p_F^2 - q^2)/2 \ , \tag{6}$$

if $q \leq p_F$, and zero otherwise. For $n \neq 0$

$$G_n(q) = \begin{cases} 4p_F^3 M_n/3, & q < K_n - p_F, \\ M_n[q^3/3 - K_n q^2 + (K_n^2 - p_F^2)q + 2p_F^3/3 + K_n p_F^2 - K_n^3/3], & q \in (K_n - p_F, K_n + p_F), \\ 0, & q > K_n + p_F, \end{cases} \tag{7}$$

with

$$M_n = N_n\langle 1 + \cos(\vec{K}_n\cdot\vec{\tau})\rangle/8K_n \ .$$

N_n is the number of reciprocal-lattice points in the nth shell. $\langle\cdots\rangle$ denotes an average over this shell. The vec-

tor $\vec{\tau}$ has the components $\frac{1}{2}a$, $a/2\times 3^{1/2}$, and $\frac{1}{2}c$. We have evaluated the integrals Eqs. (4) and (5) and the sum in Eq. (3) for one and two $6s$ electrons in Lu. The values p_F for the configuration $5d^26s^1$ and $5d^16s^2$ are 0.530 and 0.668 a.u., respectively. The contribution of 30 shells has been considered.

The term $n=0$ contributes 73% to the Compton profiles and the terms 1 to 30 contribute another 23%. The convergence of the sum is apparently rather slow and it would be necessary to extend the sum [Eq. (3)] to much higher values of n in order to get the remaining 4%. We have therefore multiplied the

TABLE II. Experimental Compton profiles of polycrystalline Lu (corrected for multiple scattering). Column 2 gives the total profile and column 3 the contribution of the conduction electrons obtained by subtracting the convoluted core contribution (Ref. 11). Columns 4 and 6 give the Compton profiles of the conduction electrons in the RFA model for the atomic configurations $5d^16s^2$ and $5d^26s^1$. In order to compare these with the experimental profile of the conduction electrons (column 3) they have been convoluted with the energy resolution function in columns 5 and 7.

	$J^{Lu}(q)$	$J^{Lu}_{CE}(q)$	$J^{RFA}_{5d^16s^2}(q)$		$J^{RFA}_{5d^26s^1}(q)$	
	Exp.	Exp.				
q (a.u.)	not deconvoluted	not deconvoluted	not convoluted	convoluted	not convoluted	convoluted
0.0	9.70	2.30	2.331	2.236	2.115	2.018
0.1	9.64	2.26	2.294	2.197	2.078	1.979
0.2	9.57	2.23	2.181	2.081	1.964	1.861
0.3	9.24	1.96	1.989	1.886	1.766	1.671
0.4	8.83	1.64	1.711	1.619	1.472	1.432
0.5	8.40	1.34	1.344	1.304	1.073	1.185
0.6	7.90	0.99	0.890	0.987	0.870	0.972
0.7	7.41	0.67	0.519	0.724	0.772	0.809
0.8	7.02	0.48	0.463	0.543	0.672	0.686
0.9	6.76	0.44	0.406	0.432	0.514	0.585
1.0	6.49	0.39	0.353	0.362	0.485	0.497
1.1	6.19	0.30	0.304	0.309	0.407	0.417
1.2	5.85	0.19	0.257	0.263	0.334	0.347
1.3	5.58	0.13	0.216	0.221	0.274	0.285
1.4	5.34	0.11	0.179	0.184	0.222	0.232
1.5	5.20	0.13	0.146	0.151	0.178	0.188
1.6	5.08	0.12	0.117	0.123	0.142	0.151
1.7	4.89	0.12	0.093	0.099	0.113	0.120
1.8	4.71	0.11	0.074	0.080	0.092	0.095
1.9	4.58	0.11	0.060	0.064	0.073	0.076
2.0	4.48	0.12	0.049	0.052	0.059	0.061
2.2	4.23	0.08	0.033	0.035	0.039	0.041
2.4	4.02	0.03	0.022	0.024	0.024	0.027
2.6	3.83	0.00	0.017	0.017	0.019	0.019
2.8	3.66		0.012	0.012	0.014	0.014
3.0	3.53		0.008	0.009	0.009	0.009
3.2	3.35		0.006	0.006	0.006	0.006
3.4	3.20		0.004	0.004	0.005	0.005
3.6	3.10		0.003	0.003	0.004	0.004
3.8	2.95		0.002	0.002	0.004	0.004
4.0	2.82		0.002	0.002	0.004	0.003
4.2	2.65		0.002	0.002	0.003	
4.4	2.47		0.002	0.002	0.003	
4.6	2.34				0.003	
4.8	2.24					
5.0	2.09					
5.2	1.99					
5.4	1.86					
5.6	1.74					
5.8	1.70					
6.0	1.61					

contribution of the shells 1 to 30 by $\frac{27}{23}$ and guaranteed by this that

$$\int_{-\infty}^{\infty} J_{6s}(q)\,dq = \begin{cases} 1 \text{ for } 6s^1, \\ 2 \text{ for } 6s^2 \end{cases} . \tag{8}$$

This is a good approximation especially in the q range between 0 and p_F. For the $5d$ electrons we have taken the atomic Compton profiles by Biggs *et al.*[11] The Compton profiles for the configurations $5d^26s^1$ and $5d^16s^2$ are listed in Table II. After adding the core contribution and convoluting with the spectrometer resolution function (Eq. 2) we have plotted in Fig. 2 the Compton profiles for these two configurations. The figure shows also the Compton profile for Lu when the three conduction electrons are treated as free electrons. It is seen that the $5d^16s^2$ configuration gives a calculated Compton profile in good agreement with the experimental data. This result is, however, in disagreement with thermochemical data[16] and theoretical calculations based on the atomic sphere approximation method.[17] The authors of both papers suggest that lutetium has a $5d^{1.5}6s^{1.5}$ configuration. This difference in electronic configurations is not too surprising considering some of the approximations made in calculating the theoretical Compton profiles.

It can be argued that renormalizing the $5d$ electron wave functions would not change the conclusion that the Compton profile experiments support a $5d^16s^2$ configuration. As shown in Fig. 2 in the case of the free electrons, $J(0)$ is larger than the experimental value because the free electrons are not bonded strongly enough. On the other hand, in the $5d^26s^1$ configuration the electrons are bonded too strongly because $J(0)$ lies below the experimental Compton profile. If one renormalized the $5d$ electrons in addition to the renormalized $6s$ electrons, the $5d$ electrons would be bonded even more strongly and thus the corresponding $J(0)$ would be shifted downward. The $J(0)$ for the $5d^16s^2$ configuration will still be in better agreement than that for the $5d^26s^1$ configuration.

The availability of an accurate band structure from which a more precise theoretical profile could be calculated might give better agreement with the $5d^{1.5}6s^{1.5}$ electronic configuration reported by others. To date only the relativistic APW band-structure calculation of Keeton and Loucks is available,[18] which, however, is not sufficiently accurate. We hope that our data will stimulate further calculations.

We now turn to the discussion of the difference profile for $LuH_{2.05}$ and Lu which is shown in Fig. 3. Compton profiles of Lu dihydride which are based on band-structure calculations have not been published. But Switendick[6] has calculated the band structure of several other rare-earth dihydrides with the CaF_2 structure. LuH_2 has this structure with a lattice constant of $a = 9.5106$ a.u.[5] The main result of these calculations is that in the dihydrides a new band is added below the Fermi level. This band corresponds to the antibonding hybrid of the two hydrogen $1s$ orbitals on the two tetrahedral sites in the unit cell. It can accommodate two electrons per atom and that is why the Fermi level is roughly unchanged during the formation of the dihydrides. A rigid-band model is therefore inadequate for the dihydride. Thus we propose the following model for LuH_2. The hydrogen atoms occupy all tetrahedral sites in the fcc lattice of lattice parameter a and form a simple cubic lattice of spacing $\frac{1}{2}a$. This hydrogen lattice will now be treated in the RFA model. We first construct antibonding wave functions $\phi(r)$ in each Wigner-Seitz sphere starting with atomic hydrogen wave functions

$$\phi(r) = A\,\pi^{-1/2}[\exp(-r) - \exp(-2r_0 + r)] , \tag{9}$$

inside $r_0 = \frac{1}{4}a$ and zero outside. For $A = 1.2806$ this function is renormalized to one within a sphere of radius r_0. The Fourier transforms $\psi_0(K_n)$ can be calculated analytically

$$\psi_0(0) = 2^{1/2}(\pi A)^{-1}[2 - 2(r_0^2 + 2)\exp(-r_0) + 2\exp(-2r_0)] , \tag{10}$$

$$\psi_0(K_n) = 2 \times 2^{1/2}(\pi A K_n)^{-1}\{K_n(1+K_n^2)^{-2}[1+\exp(-2r_0)] - \exp(-r_0)(1+K_n^2)^{-1}[r_0 \sin K_n r_0 + K_n(1+K_n^2)^{-1}\cos K_n r_0]\} . \tag{11}$$

The factor $G_n(q)$ entering the Compton profile Eq. (3) is again given by Eqs. (6) and (7). Here $M_n = N_n/4K_n$ and $p_F = 0.651$ a.u. It turned out that the sum in Eq. (3) converges rapidly. Only terms up to $n = 3$ have to be considered. The result of this calculation is shown in Fig. 3 after convolution with the energy resolution function Eq. (2) and in Table III. In view of the simplicity of the model used the agreement with the experimental result is good. The Lu is treated in the present model of LuH_2 merely as a fcc lattice which determines the symmetry of the hydrogen lattice and its lattice spacing. In reality, in addition to the formation of the new band, the wave functions of the Lu conduction electrons hybridize with the bonding hydrogen-hydrogen hybrids,[6] and accounts for the tenfold decrease in the density of states at the Fermi surface when the electronic specific-heat constants of Lu and LuH_2 are compared.[7] This effect needs to be taken into account if a better agreement with the experimental data should

TABLE III. Experimental difference profile between $LuH_{2.05}$ and Lu in comparison with a RFA and a protonic model outlined in the text.

	$J_{LuH_{2.05}}(q) - J_{Lu}(q)$			
q (a.u.)	Exp. not deconvoluted	RFA not convoluted	RFA convoluted	Protonic model not deconvoluted
0.0	0.96	1.144	1.106	1.57
0.1	0.97	1.129	1.091	1.54
0.2	1.00	1.083	1.045	1.52
0.3	1.02	1.007	0.970	1.34
0.4	1.00	0.900	0.870	1.12
0.5	0.95	0.762	0.757	0.92
0.6	0.85	0.594	0.648	0.68
0.7	0.75	0.497	0.562	0.46
0.8	0.64	0.488	0.504	0.33
0.9	0.52	0.468	0.466	0.30
1.0	0.41	0.440	0.434	0.27
1.1	0.32	0.406	0.400	0.21
1.2	0.24	0.368	0.363	0.13
1.3	0.17	0.325	0.321	0.09
1.4	0.12	0.279	0.278	0.08
1.5	0.09	0.231	0.233	0.09
1.6	0.07	0.184	0.189	0.08
1.7	0.06	0.141	0.148	0.08
1.8	0.06	0.104	0.113	0.08
1.9	0.07	0.075	0.085	0.08
2.0	0.07	0.057	0.063	0.08
2.2	0.06	0.030	0.033	0.05
2.4	0.05	0.011	0.015	0.02
2.6	0.05	0.005	0.006	0.00
2.8	0.05	0.003	0.003	
3.0	0.03	0.003	0.002	
3.2	0.01	0.002	0.002	
3.4	0.01	0.002	0.002	
3.6	0	0.002	0.002	

be obtained. But, apparently the antibonding hybrids of the $1s$ hydrogen wave functions are the essential feature in the electronic structure of this dihydride as suggested by Switendick. Figure 3 shows also the difference Compton profile $\Delta J(q)$ for the dihydride under the assumption that the hydrogen electrons increase the momentum distribution of the conduction electrons in metallic Lu according to their increased number

$$\Delta J(q) = \frac{2.05}{3} J_{CE}(q) \ , \tag{12}$$

where $J_{CE}(q)$ is the Compton profile for the three conduction electrons of Lu from Table II. This model is called "protonic" in the figure. It is clearly seen that at low $|q|$ values, <1, the band-structure calculation by Switendick, labeled "RFA model", gives a much better fit than the protonic model. At high $|q|$ values, $|q| > 1$, the experimental data are not able to discriminate between the two models.

Furthermore, it is noted that as $q \rightarrow 0$, neither model has the correct shape. The differences between the RFA model and experimental results, may be in part due to some of the difficulties noted above in our discussion concerning Lu metal. Another possible reason for the discrepancy is that we have assumed all of the hydrogen atoms occupy the tetrahedral sites, but other experimental data suggest that some of the octahedral sites (anywhere from 2 to 10%) are occupied.[19] Since the fractional occupation values are not available, we have made no attempt to take octahedral site occupancy into account in calculating the Compton profile.

In summary, the Compton profile measurements suggest a $5d^1 6s^2$ electronic configuration for Lu metal and that Switendick's band structure for the RH_2 compounds is qualitative correct for LuH_2.

ACKNOWLEDGMENTS

The authors would like to thank Dr. J. Felsteiner for kindly giving us the Monte Carlo program used to make the corrections for multiple scattering. A portion of this work was supported by the U. S. DOE, Office of Basic Energy Sciences, Division of Materials Sciences.

---

[1]B. Williams, *Compton Scattering* (McGraw-Hill, New York, 1977), and the references therein.

[2]J. A. Hoekstra and R. A. Phillips, Phys. Rev. A 4, 4184 (1971).

[3]S. Berko and J. S. Plaskett, Phys. Rev. 112, 1877 (1958).

[4]K. F. Berggren, S. Manninen, and T. Paakkari, Phys. Rev. B 8, 2516 (1973).

[5]G. G. Libowitz, *The Solid-State Chemistry of Binary Metal Hydrides* (Benjamin, New York, 1965).

[6]A. C. Switendick, Int. J. Quantum Chem. 5, 459 (1971), and in *Hydrogen Energy,* edited by T. N. Veziroglu (Plenum, New York, 1975), Vol. 2, p. 1029.

[7]D. K. Thome, K. A. Gschneidner, Jr., G. S. Mowry, and J. F. Smith, Solid State Commun. 25, 297 (1978).

[8]R. Lässer and B. Lengeler, Phys. Rev. B 18, 637 (1978).

[9]G. L. Borchert, W. Scheck, and K. P. Wieder, Z. Naturforsch. A 30, 274 (1975).

[10]Throughout this paper lengths and momenta are given in atomic units: a_0 (Bohr radius) for length and $\hbar/a_0$ for momentum.

[11]F. Biggs, L. B. Mendelssohn, and J. B. Mann, At. Data Nucl. Data Tables 16, 201 (1975).

[12]J. Felsteiner and P. Pattison, Nucl. Instrum. Methods 124, 449 (1975).

[13]F. Herman and S. Skillman, *Atomic Structure Calculations* (Prentice-Hall, Englewood Cliffs, 1963).

[14]F. H. Spedding and B. J. Beaudry, J. Less-Common Met. 25, 61 (1971).

[15]K. F. Berggren, S. Manninen, T. Paakkari, O. Aikala, and K. Mansikka, in Ref. 1, p. 139.

[16]K. A. Gschneidner, Jr., J. Less-Common Met. 25, 405 (1971).

[17]J. C. Duthie and D. G. Pettifor, Phys. Rev. Lett. 38, 564 (1977).

[18]S. C. Keeton and T. L. Loucks, Phys. Rev. 168, 672 (1968).

[19]G. G. Libowitz and A. J. Maeland, in *Handbook on the Physics and Chemistry of Rare Earths,* edited by K. A. Gschneidner, Jr. and L. Eyring (North-Holland, Amsterdam, 1979), Vol. 3, p. 299.